Laboratory measurements of stomatal NO_2 deposition to native California trees and the role of forests in the NO_x cycle

Erin R. Delaria[1], Bryan K. Place[1], Amy X. Liu[1], and Ronald C. Cohen[1, 2]

[1]Department of Chemistry, University of California Berkeley, Berkeley, CA, USA
[2]Department of Earth and Planetary Science, University of California Berkeley, Berkeley, CA, USA

Correspondence: Ronald C. Cohen (rccohen@berkeley.edu)

Abstract.

Both canopy-level field measurements and laboratory studies suggest that absorption of NO_2 through the leaf stomata of vegetation is a significant sink of atmospheric NO_x. However, the mechanisms of this foliar NO_2 uptake and their impact on NO_x lifetimes remains incompletely understood. To understand the leaf-level processes affecting ecosystem scale atmosphere-

5   biosphere NO_x exchange, we have conducted laboratory experiments of branch-level NO_2 deposition fluxes to six coniferous and four broadleaf native California trees using a branch enclosure system with direct Laser Induced Fluorescence (LIF) detection of NO_2. We report NO_2 foliar deposition that demonstrates a large degree of inter-species variability, with maximum observed deposition velocities ranging from $0.15 – 0.51$ cm s^{-1} during the daytime, as well as significant stomatal opening during the night. We also find that the contribution of mesophyllic processing to the overall deposition rate of NO_2 varies by

10   tree species, but has an ultimately inconsequential impact on NO_x budgets and lifetimes. Additionally, we find no evidence of any emission of NO_2 from leaves, suggesting an effective uni-directional exchange of NO_x between the atmosphere and vegetation.

1 Introduction

Nitrogen oxides ($NO_x \equiv NO + NO_2$) are a form of reactive nitrogen that plays a major role in the chemistry of the atmosphere.

15   NO_x catalyzes tropospheric ozone formation, contributes to the production of photochemical smog, and influences the oxidative capacity of the atmosphere (Crutzen, 1979). NO_x is primarily emitted as NO through fossil fuel burning, lighting, and soil microbial activity. The latter source is of particular importance in remote, forested, and agricultural regions.

Understanding the fate of atmospheric NO_x, in addition to its emission sources, is essential for interpreting the impact of NO_x on atmospheric chemistry. Prior studies have demonstrated that NO_2 can directly deposit to foliage via diffusion through

20   stomata (e.g., Teklemmariam and Sparks, 2006; Chaparro-Suarez et al., 2011; Breuninger et al., 2013; Delaria et al., 2018). The currently understood mechanism of this uptake process is as follows: NO_2 enters through the stomatal cavity and dissolves into the apoplastic fluid, forming nitrate, which then is reduced to ammonium by the enzyme nitrate reductase (Park and Lee, 1988; Ammann et al., 1995; Tischner, 2000; Lillo, 2008; Heidari et al., 2011). There is evidence that NO_2 may also be directly scavenged by antioxidants, most notably ascorbate (Ramge et al., 1993; Teklemmariam and Sparks, 2006). These processes

25 may be impacted by the leaf pH, which is known to change under conditions of limited water availability (Bahrun et al., 2002).
Experiments using ^{15}N as an isotopic tracer have demonstrated that absorbed NO_2 is eventually assimilated into amino acids
(Rogers et al., 1979; Okano and Totsuka, 1986). Although the role of stomatal conductance (g_s) in controlling the deposition
of NO_2 is well-documented, the impact of the processes in the mesophyll–processes taking place between the intercellular air
space and the ultimate nitrogen assimilation site–on the rate of uptake remains poorly resolved. The question of whether and
30 how much mesophyllic processes affect NO_x budgets at the canopy scale thus persists.

The most divisive example of the mesophyll quandry is the sometimes-reported emission of NO_x from plants, mostly in the
form of NO, at low NO_x mixing ratios that would be relevant to remote forested regions (Johansson, 1987; Rondón and Granat,
1994; Hereid and Monson, 2001; Sparks et al., 2001; Teklemmariam and Sparks, 2006). This would, under many conditions,
indicate that trees instead serve as a constant source, rather than sink, of NO_x. However, this idea has been called into question
35 by a number recent studies including Lerdau et al. (2000), Chaparro-Suarez et al. (2011), Breuninger et al. (2013) and Delaria
et al. (2018). It is possible that the magnitude and direction of the NO_x flux to leaves may vary depending on the species
and conditions. One such factor that has been suggested to impact foliar emission and deposition of NO_x is elevated soil
nitrogen. Soil nitrate fertilization has been documented to lead to an increase in nitrate reductase activity in the needles of scots
pine seedlings (Andrews, 1986; Pietilainen and Lahdesmaki, 1988; Sarjala, 1991). It is possible that as a result of abundant
40 nitrate fertilization, nitrate accumulates in leaves, leading to emission or a reduction in uptake. For example, Chen et al. (2012)
observed an increase in NO emission and Teklemmariam and Sparks (2006) detected an increase of NO_2 emission under
conditions of elevated soil nitrate. *Per contra*, Joensuu et al. (2014) found no evidence of fertilization-induced NO_x emissions.
No influence of soil nitrogen on either NO_2 or NO uptake has been documented at atmospherically relevant conditions (Okano
and Totsuka, 1986; Teklemmariam and Sparks, 2006; Joensuu et al., 2014).

45 In this study we present results from laboratory measurements of NO_2 fluxes on ten native California tree species–six conifers
and four broadleaf trees–using a branch enclosure system and laser-induced fluorescence (LIF) detection of NO_2. Here we
investigate the relative influence of stomatal and mesophyllic processes on the total uptake rate of NO_2 under atmospherically
relevant conditions. Our aim is to assess the factors controlling NO_2 foliar deposition and their ultimate impact on the NO_x
cycle. To test this, we measured the NO_2 deposition velocity over a range of stomatal conductances and considered evidence
50 for additional limits on the uptake rate. We also conducted experiments under drought and elevated soil nitrogen and tested for
indications of an NO_2 compensation point or changes in the apparent mesophyllic uptake limit.

2 Methods

2.1 Tree specimens

Foliar deposition of NO_2 was investigated in the laboratory using ten native California tree species–*Pinus sabiniana, Pinus
55 ponderosa, Pinus contorta, Pseudotsuga menziesii, Calocedrus decurrens, Sequoia sempervirens, Arbutus menziesii, Acer
macrophyllum, Quercus agrifolia, and Quercus douglasii*. Three to six individuals of each species were purchased from a local
native California plant nursery (Native Here Nursery) or Forestfarm, where the plants were grown from seeds and cuttings.

The tree specimens were grown in a nutrient-rich commercial soil mixture of Sun Gro Sunshine #4 and Supersoil potting soil in 20—40 liter pots in an outdoor section of the Oxford facility greenhouse at the University of California, Berkeley. The trees were 2—3 years old when measurements were taken. No additional fertilizers or pesticides were used on the plants. Trees were transported into the lab for experimentation, where they were exposed to a 12 h light/dark cycle. Trees were illuminated with an LED diode array of 430—475 and 620—670 nm lights (Apollo Horticulture). For the deciduous trees (*Q. douglassi, and A. macrophyllum*) experiments were run between May and September 2019. For all other species experiments were conducted year-round, between October 2018 and November 2019.

2.2   LIF measurement of NO$_2$ deposition fluxes

Measurements were made with a dynamic chamber and Laser-Induced Fluorescence (LIF) detection of NO$_2$. A full description of our apparatus can be found in Delaria et al. (2018). Briefly, an NO$_2$ standard was mixed with humidified zero air (air filtered to remove NO$_x$ and reactive species) and delivered to a ~10 L chamber enclosing the branch of a tree at a total flow rate of ~6000 cm^3 min^{-1} (Fig.1). The lifetime of air within the chamber was $\sim$ 2 min. Humidity was adjusted by controlling the fraction of zero air that passed through a bubbler filled with distilled water. The mixing ratios of NO$_2$ entering the chamber were typically between 0—10 ppb. Some of the air entering the chamber was diverted to cell #1 of the NO$_2$ LIF analyzer and two Licor instruments (6262 and 7000) for measuring the mixing ratios of NO$_2$ and H$_2$O/CO$_2$, respectively in the inflowing air stream, such that the flow rate of air directly into the chamber was ~5000 cm^3 min^{-1}. Air from the chamber was simultaneously pumped out to cell #2 of the NO$_2$ LIF analyzer and the Licor-7000 instrument for measuring the mixing ratio of NO$_2$ within the chamber and the change in CO$_2$ and water vapor between the in- and outgoing air streams, respectively (Fig. 1). A slight positive pressure was maintained within the chamber to ensure lab air did not leak into the chamber.

Fluxes of NO$_2$ to leaves were calculated according to (Eq. 1—2):

$$Flux = \frac{Q}{A}([NO_2]_{in} - [NO_2]_{out}) \tag{1}$$

$$Flux = V_d([NO_2]_{out} - [NO_2]_{comp}) \tag{2}$$

where [NO$_2$]$_{in}$ and [NO$_2$]$_{out}$ are concentrations of NO$_2$ entering and exiting the chamber, respectively, [NO$_2$]$_{comp}$ is the compensation point concentration, Q is the flow rate (cm^3/s), A is the enclosed one-sided leaf area, and V_d is the deposition velocity. The leaf area was determined using the ImageJ software package (Schneider and Eliceiri, 2012) and the flow rate was measured at the beginning of each experimental run (Mesa Laboratories 510-M Bios Defender). Peroxyacetyl nitrate (PAN) and acetone were also delivered to the chamber for simultaneous measurements of PAN stomatal deposition. Negligible thermal production of NO$_2$ was observed. The results of PAN deposition experiments will be discussed elsewhere. The NO$_2$ mixing ratio was also corrected for the differences in collisional quenching of the excited state NO$_2$ by water vapor in cells #1 and #2, caused by transpiration of the tree within the chamber (Thornton et al., 2000).

$$[NO_2]_{out,actual} = [NO_2]_{out,measured} \times (1 + 5\Delta X_{H_2O}) \tag{3}$$

90   where ΔX_{H_2O} is the difference in the water vapor mole fraction between the chamber and the incoming air stream.

     Deposition velocities were determined using the method described in Delaria et al. (2018): a weighted orthogonal distance linear regression was performed on NO_2 fluxes (determined using Eq. 1) against $[NO_2]_{out}$ to obtain a slope equal to V_d. A positive x-intercept was interpreted as evidence for a possible compensation point. During each day of experimentation we stepped through at least 8 different NO_2 concentrations, with each concentration step lasting for 40 minutes. Uncertainty in V_d

95   was obtained through propagating uncertainty in measured NO_2 concentrations, Q, and A. The uncertainty in NO_2 concentrations was estimated as one standard deviation of variation in measurements during the last 10 minutes of each concentration step. The uncertainty in Q was estimated as <1 % and a 10% uncertainty was estimated for the enclosed one-sided leaf area.

     The deposition velocities measured can be related to the resistance-model framework for deposition of trace gases developed by Baldocchi et al. (1987) (Eq.4—6).

$$100 \quad V_d = \frac{1}{R} \tag{4}$$

$$R = R_a + R_b + R_{leaf} \tag{5}$$

$$\frac{1}{R_{leaf}} = \frac{1}{R_{cut}} + \frac{1}{R_s + R_m} \tag{6}$$

105   R is the total resistance to deposition, R_a is the aerodynamic resistance, R_b is the boundary layer resistance and R_{leaf} is resistance to uptake by the leaf. R_a was assumed to be negligible under our chamber conditions (Pape et al., 2009; Breuninger et al., 2012; Delaria et al., 2018). R_{leaf} is made up of R_{cut}, R_s, and R_m. Respectively, these refer to the cuticular resistance (resistance to deposition to the surface of the leaf), stomatal resistance ($1/g_s$), and mesophyllic resistance (resistance associated with all processes taking place within the leaf that limit uptake).

2.3   Measurement of stomatal conductance

CO_2 and water vapor exchanges were measured using the Licor 6262 and Licor 7000 instruments. Measurements of water vapor exchange were used to calculate the transpiration rate (E) and total conductance to water vapor (g_t^w) using Eq. 7 and Eq. 8, according to von Caemmerer and Farquhar (1981).

$$E = \frac{Q}{A} \frac{w_a - w_e}{1 - w_a} \tag{7}$$

115

$$g_t^w = \frac{E(1 - (w_i + w_a)/2)}{w_i - w_a} \tag{8}$$

where w_a and w_e are the mole fractions of water vapor of the outgoing and incoming airstreams, respectively, and ω_i is the internal leaf water vapor mole fraction. ω_e was measured with the Licor-6262 with dry air as a reference and $\Delta\omega(\omega_a - \omega_e)$

was measured with the Licor-7000 with incoming air as the reference. ω_i was assumed to be the saturation vapor pressure at
the leaf temperature, which was measured with a thermocouple at the surface of an enclosed leaf. The chamber temperature
was measured with a second thermocouple and was typically $20\pm3°C$. The photosynthetic photon flux density (PPFD) was
monitored outside the chamber with a LiCor quantum sensor (LiCor LI-190SA) and was $1190\,\mu mol\ m^{-2}\ s^{-1}$, approximately
the PPFD for Berkeley, California, at noon during the month of October. We performed calculations based on von Caemmerer
and Farquhar (1981) to confirm this is above the photon flux required to achieve maximal stomatal aperture for tree types
relevant to this study. Total conductance was calculated as the average over the light or dark period of an experiment. The un-
certainty in our calculation of total conductance to water vapor was primarily influenced by uncertainty in the leaf temperature
and the assumption of leaf water vapor saturation. We observed fluctuations in the temperature of enclosed leaves of $\pm2°C$.
Total uncertainty in g_t^w was determined by propagating this uncertainty in leaf temperature, which resulted in larger estimated
uncertainties at larger chamber humidities, usually coinciding with higher stomatal conductances. Chamber relative humidity
was maintained at less than 90% to minimize this effect. Variations in stomatal conductance were achieved by varying the mole
fraction of water vapor in the air delivered to the chamber. The Licor-6262 instrument was calibrated weekly using standard
CO_2 cylinders and the Licor-610 dewpoint generator. The Licor-7000 instrument was calibrated daily.

The stomatal conductance (g_s^w) could then be calculated from Eq. 9:

$$\frac{1}{g_s^w} = \frac{1}{g_t^w} - \frac{1}{g_b^w} \tag{9}$$

where $1/g_b^w$ is the boundary layer resistance to water vapor. The boundary layer resistance to water vapor was estimated to be
negligible under our experimental conditions, with an upper bound of $0.6\ s\ cm^{-1}$ determined using the methods described by
Delaria et al. (2018). Stomatal (g_s) and total (g_t) conductances to NO_2 were calculated by scaling the values for water vapor
by the ratio of diffusivities in air (D_{NO_2}/D_{H_2O}) according to Massman (1998).

2.4 Nitrogen measurements

To test the influence of excess soil nitrogen on the ability of trees to take up nitrogen through their stomata in the form of NO_2,
we fertilized three individuals of both *Quercus agrifolia* and *Pseudotsuga menziesii* with a 20 mM ammonium nitrate soilution.
The trees were watered with 250 ml of this ammonium nitrate solution three days per week. Three individuals of each species
were watered with DI water as the control group. The trees underwent this fertilization treatment for 120 days before beginning
dynamic chamber measurements on NO_2 foliar deposition. NO_2 deposition experiments were conducted for 70 days, during
which time the soil fertilization treatments were continued.

2.4.1 Soil nitrogen

Approximately 5 mg of a soil core sample was taken each day from the individual on which we conducted an NO_2 deposition
experiment. The soil was sifted through a mesh 2 mm sieve. Soil nitrate and ammonium were extracted by shaking ≈2.5 mg
of the soil sample in 30 ml of $\approx$ 2M KCl for one hour, followed by filtering the samples through a Whatman No.1 filter paper.
The other ≈2.5 mg was dried in a drying oven at 60°C for at least 48 hours. The mass of the soil after drying was measured to

determine the percentage dry mass of the extracted soil sample. Six KCl blanks, 3 KCl samples spiked with 5 mL (low QC), and 3 KCl samples spiked with 10 mL KCl (high QC) were carried through the extraction process to serve as quality controls (QC samples). NH_4^+ and NO_3^- were measured using a colorimetric synthesis following the method of Sims et al. (1995) and Decina et al. (2017). Briefly, a standard 1 ppm stock solution of ammonium nitrate was made from ammonium nitrate solid dissolved
155 in milli-q water, and was diluted to 0, 0.1, 0.2, 0.3, 0.4, and 0.5 mg/L in 1 cm, 2.5 mL cuvettes. These standard solutions served as the calibration standards; we made three sets of calibration standards for both ammonium and nitrate analysis. All glassware was acid washed in a 1M solution of HCl prior to all measurements and extractions to prevent contamination.

For ammonium analysis, 160 μL of each soil extraction sample from the control group, 10 μL from the fertilizer-treated group, and 1.6 mL of the QC samples were pipetted into individual cuvettes. 100, 200, 100, and 500 μL of 0.2 M citrate, 5
160 mM nitroprusside, 0.3 M hypochlorite reagents, and milli-q water, respectively, were then added sequentially into each cuvette. The cuvettes were filled to a final volume of 2.5 mL with KCl, and the samples were allowed to sit for 30 min. For nitrate measurements, 320 μL and 10 μL of soil samples from the the control and fertilized groups, respectively, and 1550 μL of the QC samples, were pipetted into separate cuvetts. 950 μL of a regent containing 1g/L vanadium chloride and 25 mg/L N-(1-Naphthyl)ethylenediamine (NEDD) was subsequently added to each cuvette, which were then filled to a final volume of 2.5
165 mL with KCl and allowed to sit for 24 hrs. 160 μL and 320 μL of a control *Q. agrifolia* soil extraction sample were added to one set of calibration standards for ammonium and nitrate analysis, respectively, to test the effects of the soil matrix on the calibration.

Concentrations of ammonium and nitrate in each sample were determined with colorimetric measurements using a custom built spectrophotometer. The spectrophotometer light source was a broad spectrum quartz tungsten-halogen lamp (QTH10
170 Thorlabs Inc.). The absorption of each sample and standard was measured with the light source passing through a 540 ± 2 nm bandpass filter (FB570-10 Thorlabs Inc.) for nitrate analysis or a 670 ± 2 nm bandpass filter (FB540-10 Thorlabs Inc.) for ammonium analysis.

2.4.2 Uncertainty analysis

Concentrations of ammonium and nitrate in the soil extraction samples were determined from the slope in their respective
175 calibration curves. The calibrations for ammonium and nitrate analysis had respective uncertainties of 7% and 5%. The slopes of the calibration curves with added sample from a *Q. agrifolia* soil extraction were not statistically different from those containing only standards, allowing us to exclude the possibility of interference from the soil matrix.

The accuracy uncertainty in the high and low QC samples were 3% and 11%, respectively for anmmonium measurements, and 3% and 12% for nitrate measurements. We estimated the resulting uncertainty for cuvette samples with less than 0.15 mg/L
180 NH_4^+ or NO_3^- ($\approx$ 1.8 μg/mg soil NH_4^+ or NO_3^-) to be 15%. Samples with larger concentrations were estimated to have 5% uncertainty. The blank quality control standards contained 0.04 mg/L ammonium and nitrate. This was blank-subtracted from each sample.

2.4.3 Leaf nitrogen

After deposition experiments were completed the leaves were removed from the trees and dried for 48 hours in a drying oven.
185   The leaves were then ground to a fine powder and the percent nitrogen, hydrogen, and carbon content were measured with a
ICP Optima 7000 DV instrument.

2.5 Drought stress

Calocedrus decurrens and *Pinus ponderosa* were drought stressed to study the impact of drought on NO_2 deposition. Three
individuals of each species were watered daily (control group) and three individuals of each species were watered with 250
190   mL once every four weeks (drought group). Limited-water treatment of the drought group was carried out for 60 days before
conducting dynamic chamber experiments for NO_2 foliar deposition. NO_2 deposition experiments were run for 30-40 days.
During the experiments, the control group was watered 50 mL daily and the experimental group was watered 50 mL once every
two weeks. The *P. ponderosa* drought-stress experiments took place between March and June 2019. The *C. decurrens* drought
stress spanned from August to December 2019.
195   The xylem water potential (Ψ_p) of the trees were monitored to measure the drought stress level of the trees using a Scholan-
der pressure chamber (Model 670 PMS Instr. Comp.). Leaves were cut, wrapped in aluminum foil, and then inserted into the
pressure bomb. The Ψ_p of cuttings were measured around 11:00AM each day. A Ψ_p measurement lower than -1.0 MPa indi-
cated signs of drought stress in the *P. ponderosa*. The *C. decurrens* did not show evidence of drought stress in Ψ_p measurements
while in the greenhouse, however, early signs of embolism were observed.

200   ## 3 Results

V_d was calculated for each day of measurements with a weighted linear regression of measured fluxes and chamber NO_2
concentrations (Delaria et al., 2018). No statistically significant compensation point was observed under any experimental
condition for the majority of the species studied, in agreement with previous work (Chaparro-Suarez et al., 2011; Breuninger
et al., 2013; Delaria et al., 2018). Only *P. menziesii* was found to have a compensation point, estimated to be 20 ppt, but this
205   concentration is below the limit of quantification for our instrument and we believe this measurement to be consistent with a
compensation point of zero. V_d and g_s measurements allowed for consideration of whether the deposition of NO_2 is exclusively
stomatally controlled, or is also affected by the internal processing in the mesophyll. We rarely observed total closing of the
stomata when the chamber lights were turned off at night. All of the deposition observed at night could be explained by
deposition to these partially open stomata. This is consistant with previous studies observing only partial closing of stomata at
210   night in a variety of plant species (Dawson et al., 2007; Drake et al., 2013) . The results of experiments are show in (Table 2).

3.1 Measurements of mesophyllic resistance

We utilized two methods of examining the importance of the mesophyllic resistance on the deposition of NO_2. Figure 2 shows the predicted stomatal-limited NO_2 deposition fluxes, assuming negligible R_b and R_m ($Flux = g_t[NO_2]_{out}$) plotted vs. the measured NO_2 fluxes. Our upper bound measurement of R_b for NO_2 is 1 s cm^{-1} (0.6 s cm^{-1} for water vapor). This was

215   calculated by measuring the deposition of NO_2 to a 30 cm^2 tray of activated charcoal. R_b decreases with the enclosed leaf area according to Pape et al. (2009), which at a minimum was 200 cm^2. The maximum R_b in the chamber should thus be $\approx$0.1 s cm^{-1}. Assuming $g_s = g_t$ would lead to a maximum of a 6% error in the calculated g_s assuming a g_t of 0.6 cm s^{-1} and R_b of 0.1 s cm^{-1}. Any deviation from unity in the observed slope of predicted vs. measured fluxes can thus be attributed to R_m. Significant deviations from unity can be seen in several species, most notably *S. sempervirens* (Table 2 and Fig. 2). Slopes

220   were calculated using a weighted average of the slopes obtained from a least squares cubic weighted fit of each individual experiment (Table 2). Some experiments were excluded (shown in red in Fig. 2), as they were determined to be outliers by a generalized extreme studentized deviate test for outliers. Identified outliers were excluded both to account for potentially erroneous deviations in the V_d/g_t ratio (most likely due to systematic error in calibration of the Licor-7000 instrument), and to avoid over-weighting of days with abnormally large stomatal conductances. These latter instances normally coincided with

225   low V_d/g_t ratios, and if these data were also subject to some systematic error, would bias our analysis of R_m.

R_m was also explicitly calculated using the relationship of V_d and g_t. Figure 3 shows V_d from each day of experiments plotted against the measured g_t. Deviations from the 1:1 line are attributable to the mesophyllic resistance. R_m was calculated with a weighted fit of the resistance model:

$$V_d = \frac{1}{R_c} + \frac{1}{(\frac{1}{g_s} + R_m)} \tag{10}$$

230   No significant cuticular resistances were observed so only results of R_m are recorded (Table 2). R_m was calculated both assuming negligible R_b ($g_s = g_t$) and R_b = 1 s cm^{-1}. There were no significant differences between these two calculations (Table 2).

3.2 Effects of excess soil nitrogen

The impact of soil fertilzation on the foliar uptake of NO_2 by two tree species, *Q. agrifolia* and *P. menziesii*, was examined

235   by watering a control group of both species with deionized water and a fertilized group with 20 ppm ammonium nitrate. On average, the soil nitrogen concentrations of NH_4^+ and NO_3^- were 100x larger for the fertilized groups than the control groups (Table 1). The percentage of leaf nitrogen content approximately doubled between the control groups and the fertilized groups (Table 1).

The effect of soil nitrogen fertilization and leaf nitrogen content on the ratio of V_d/g_t is shown in Fig. 4. No significant

240   relationship (α = 0.01) was observed for either *Q. agrifolia* of *P. menziesii*, suggesting the mesophyllic processing of NO_2 is unaffected by soil or leaf nitrogen content. We also observe no increase in the compensation point of NO_2 as a result of higher

leaf nitrogen content or elevated soil nitrogen (Fig. 5). The trees on which we conducted these experiments were observed to behave consistently up to the point of embolism.

3.3 Drought stress measurements

245 The impact of drought stress on NO_2 foliar uptake for *C. decurrens* and *P. ponderosa* was observed by regularly watering a control group and watering an experimental, drought group at much lower frequency (once every 4 weeks in the greenhouse, and once every 2 weeks in lab). The median Ψ_p measured was lower for the drought groups than the control groups (Table 3), *C. decurrens* drought median Ψ_p was -0.80 MPa compared to control median of -0.30 MPa, and *P. ponderosa* drought median was -1.05 MPa compared to control median of -0.60 MPa. The first quartiles of the control groups and third quartiles of the

250 drought groups do not overlap, reflecting a significant difference between the Ψ_p measurements of the two groups. We also observed a strong correlation between measured Ψ_p and stomatal conductance. We find a more substantial impact of drought on the water potentials, and of the water potentials on the stomatal conductance, in *P. ponderosa* trees than *C. decurrens*. Both these California conifer species are quite drought resistant (Pharis, 1966; Kolb and Robberecht, 1996; Maherali and DeLucia, 2000), but these results may indicate *C. decurrens* is particularly protected against water loss.

255 The mesophyllic resistance (R_m) calculated showed a statistically significant difference for both *C. decurrens* and *P. ponderosa*. R_m in drought-stressed *C. decurrens* increased from 0.37 s cm^{-1} to 1.17 s cm^{-1}, while in *P. ponderosa* R_m decreased from 0.86 s cm^{-1} to 0 s cm^{-1}. The effects on calculated R_m are also reflected in the relationship of measured conductance (g_t) and deposition velocity (V_d) (Figure S4).

4 Discussion

260 ### 4.1 Effects of mesophyll resistance on the lifetime of NO_x

The mesophyllic resistances (R_m) for each of the ten tree species measured are calculated from Fig. 3 and Eq. 10 and are tabulated in Table 2, assuming either $g_s = g_t$ or the upper bound for R_b. The slopes of predicted fluxes vs. measured fluxes, calculated in Fig. 2, are also tabulated in Table 2. The importance of the mesophyllic resistance and internal processing of NO_2 can be evaluated by examining both R_m and the slope of measured vs. predicted fluxes. We also examined the potential

265 impact of the mesophyllic processing of NO_2 by considering the Pearson's correlation coefficient between g_t and the slope of measured vs. predicted fluxes measured on each day an experiment was run. These correlation coefficients can be found in Table 2. The more negative this correlation, the greater the deviation in the slope from unity for higher values of g_t, consistent with larger impact of the mesophyll on the NO_2 uptake rate. All tree species except for *C. decurrens*, *Q. agrifolia*, and *Q. douglasii* show statistically significant correlations ($\alpha = 0.05$) (Table 2). R_m becomes more important at larger stomatal conductances

270 (lower stomatal resistances), as can be seen with the increasing deviations from 1:1 in some species at higher values of g_t in Fig.3. Thus, even for trees with higher calculated R_m, the impact of mesophyllic processing is unlikely to be large if the maximum stomatal conductance observed is relatively small, resulting in a slope in the measured vs predicted flux that does

not deviate greatly from unity. This is the case for *Q. agrifolia* and *P. ponderosa*. Alternatively, *P. sabiniana* demonstrates a case of a relatively small R_m, but also a smaller slope in measured vs. predicted fluxes, driven by consistently larger stomatal

275   conductances (lower R_s) (Fig. 3). However, the greater uncertainty in measurements of stomatal conductance at a larger chamber humidity calls in to question the accuracy of many g_t measurements larger than approximately 0.4 cm s^{-1}.

To evaluate with greater certainty the relationship of V_d and g_t, we conducted a set of experiments in helium to raise the stomatal conductance by increasing the gas diffusivities while maintaining relatively lower chamber humidity. These experiments were conducted on four of the tree species: *P. sabiniana, S. sempervirens, Q. agrifolia, A. macrophyllum* and *A. menziesii*. In

280   these experiments the V_d/g_t ratio for *A. menziesii* and *P. sabiniana* remained close to 1:1 up to 0.4 and 1.3 cm s^{-1} stomatal conductance, respectively (Fig. 3). We therefore suspect negligible contribution of the mesophyll to deposition to these two species. The only sizable impact of mesophyllic NO$_2$ processing is seen in *S. sempervirens*, with a large calculated R_m and a frequently high g_t (Fig. 3, resulting in a slope of measured vs. predicted fluxes of 0.6–considerably below unity.

Currently, atmospheric models incorporate a mesophyllic resistance to NO$_2$ of 0.1 s cm^{-1} (Zhang et al., 2002). This would

285   result in slope of measured vs. predicted fluxes of 0.94, even with a relatively large average g_t of 0.6 cm s^{-1}. The median slope measured in our study was 0.89. Using the model presented in Delaria and Cohen (2020), we investigated whether our results could possibly imply a more important impact of the mesophyllic resistance on the atmospheric fate of NO$_x$ at the canopy level. The model was run using meteorological conditions for June measured during the BEARPEX-2009 campaign, located at a ponderosa pine forest in the western foothills of the Sierra Nevada mountain range (38°58'42.9"N, 120°57'57.9"W,

290   elevation 1315 m). The model was initialized over two days and data from the third day was analyzed. We conducted two model runs at a stomatal conductance (g_s) to NO$_2$ deposition of 0.3 cm s^{-1}–the median measured maximum stomatal conductance excluding *P.sabiniana*–with an R_m of either 0.1 or 0.6 s cm^{-1}–the median measured R_m excluding *P. sabiniana*. For a stomatal conductance to NO$_2$ of 0.3 cm s^{-1} ($\approx$ 0.5 cm s^{-1} to water vapor) the model predicts only a 2.5% decrease in NO$_x$ lost to deposition with an R_m of 0.6 compared with an R$_m$ of 0.1 s cm^{-1}. The lifetime to deposition with an R_m of 0.1 and 0.6 s

295   cm^{-1} was 30.5 hr and 32.2 hr, respectively, representing only a 6% difference. The total atmospheric lifetime of NO$_x$ in the boundary layer with an R_m of 0.1 and 0.6 s cm^{-1} was 4.86 hr and 4.89 hr, respectively, representing only a 0.6% difference. Even the observed seemingly significant mesophyllic resistance of *S. sempervirens* is therefore likely to be irrelevant at the canopy-scale. Contributions from mesophyllic processing, though mechanistically important at a cellular level, are likely to not matter at the canopy-scale. We therefore suggest that on canopy, regional, and global scales, mesophyllic processes within

300   leaves represent a negligible contribution to NO$_x$ budgets and lifetimes.

4.2   Effects of excess soil nitrogen

We observed no effects of soil nitrogen, in the form of NH$_4^+$ and NO$_3^-$, or the leaf nitrogen content on the ratio of V_d/g_t (Fig. 4) for either *Q. agrifolia* or *P. menziesii*. Changes in this ratio would indicate an effect on the mesophyllic resistance. All variation in the uptake rates (V_d) could be explained exclusively with deviations in g_t. We did observe declines in g_t in

305   the fertilized group relative to the control group during the later stages of experimentation, which coincided with observable evidence of plant stress (e.g., browning, wilting, and beginning signs of embolism). These results are supported by previous

studies which have also found a negligible impact of nitrogen fertilization on NO_2 uptake (Teklemmariam and Sparks, 2006; Joensuu et al., 2014). This suggests that the mechanism of NO_2 uptake via dissolution and subsequent reduction of NO_3^- and NO_2^- is likely not bidirectional, nor influenced by accumulation of NO_3^- and NO_2^- within the mesophyll. It seems likely that

310   either the disproportionation step and scavenging by antioxidants (e.g. ascorbate) are the rate limiting steps in the mesophyllic processing of NO_2, or that under biologically relevant conditions nitrate reductase is not saturated. This finding further supports that reactions within the mesophyll are atmospherically unimportant.

We also did not observe any evidence for a relationship between the NO_2 compensation point and the soil nitrogen content nor the leaf nitrogen content (Fig 5) for either *Q. agrifolia* or *P. menziesii*. In general, we only observed uptake and no emission

315   of NO_2. We also conducted measurements of NO uptake and emission, but the fluxes measured were so small they were below the limit of quantifcation for our instrument. Chen et al. (2012) observed a strong relationship between NO emissions from stomata and soil nitrate fertilization. However, the maximum NO emissions they measured were a factor of 50 lower than the deposition of NO_2 measured here. NO emission from leaves is therefore not likely to be a significant source of atmospheric NO_x. *P. menziessi* was the only tree examined in our experiments that demonstrated any evidence for emission of NO_2 at low

320   mixing ratios, with a compensation point of ≈ 20 ppt. This concentration is much lower than has been observed in previous studies that have detected an NO_2 compensation point (Hereid and Monson, 2001; Teklemmariam and Sparks, 2006). However, this concentration is near the limit of detection for our instrument (Delaria et al., 2018) so should be taken *cum grano salis*. A possible cause for discrepancy between our study and those that have measured significant NO_2 compensation points is that our experiments are conducted only using photosynthetically active radiation. Some past work has demonstrated that UV

325   light may cause photolysis of nitrate at the leaf surface and subsequent emission of NO_x (Hari et al., 2003; Raivonen et al., 2006). The lack of a relationship between NO_x emission and soil N fertilization contrasts with the results of Teklemmariam and Sparks (2006), but is consistent with the nitrogen fertilization experiments conducted by Joensuu et al. (2014).

4.3 Effects of drought stress

Although there was a statistically significant impact of drought stress on R_m, this is unlikely to be atmospherically relevant

330   for reasons stated above. Additionally, in the case of *P. ponderosa*, the lack of measurements at larger g_t is likely to mask any existing mesophyllic effects, leading to minimal deviation in V_d/g_t from unity (Fig. S4). Despite a calculation of significant mesophyllic resistance in both drought and control *C. decurrens* individuals, the lack of a statistically significant ($\alpha = 0.05$) correlation between g_t and V_d/g_t casts doubt on this relationship. The impact of drought on NO_2 uptake at the leaf-level is thus exclusively its affect on the stomatal conductance. At the canopy-level, documented affects of drought on leaf area also

335   requires consideration (Pharis, 1966; Kolb and Robberecht, 1996; Maherali and DeLucia, 2000).

4.4 Effects of nighttime stomatal deposition

Most atmospheric chemical transport models, such as the abundantly utilized WRF-Chem and GEOS-Chem, use the Wesley model for parameterizing dry deposition of gaseous species (e.g., Skamarock and Powers, 2008; Fast et al., 2014; Amnuay-lojaroen et al., 2014; Ng et al., 2017). These models implicitly assume the stomata are fully closed at night, despite more

340   recent studies demonstrating many species of vegetation maintain partially open stomata at night (Musselman and Minnick, 2000; Dawson et al., 2007; Fisher et al., 2007; Drake et al., 2013). We find minimal cuticular deposition of NO_2, in agreement with several other studies (Sparks et al., 2001; Chaparro-Suarez et al., 2011). However, field observations have shown that substantial nighttime deposition of NO_2 is necessary to explain nighttime levels of NO_x (Jacob and Wofsy, 1990). The same phenomenon has been seen with other gaseous molecules, most notably PAN, which has also been observed to have a non-zero

345   deposition at night (Wolfe et al., 2009; Crowley et al., 2018). Laboratory studies have measured zero PAN cuticular deposition (Sparks et al., 2003).

     To assess the impact of nighttime stomatal opening on the atmospheric fates and lifetimes of NO_x at night, we ran our 1-D multibox canopy model, under the conditions described above, at the minimum, maximum, 25th percentile, and 75th percentile of the median nighttime deposition velocities measured in this study (0.004, 0.087, 0.009, and 0.038 cm s^{-1}, respectively).

350   At such a low degree of stomatal opening, we found these deposition velocities to be statistically equivalent to the stomatal conductance to NO_2. The fractions of NO_x loss to deposition and chemistry to these levels of stomatal opening at night are shown in Fig. 6. Here chemistry represents loss to HNO_3, $RONO_2$, and PAN, and nighttime is defined from 20:00 — 05:00. The range between the first and third quartile of the nighttime deposition observed results in a range in the fraction of NO_x loss to deposition from 13% to 25% and a range in lifetime from $\approx$ 7.5—5 hrs (Fig 6).

355   The relatively large impact of the nighttime stomatal conductance on the fate of NO_x, coupled with the large degree of inter-species variation in nighttime stomatal opening, indicates a need for more extensive studies of the nighttime deposition of NO_2. Deposition is a permanent sink of atmospheric NO_x, contrasting with the major chemical nighttime sink of NO_x to PAN formation. The relative fractions of nighttime NO_x loss to deposition and PAN formation would thus be likely to have a substantial impact on the fate of atmospheric NO_x and the cycling of NO_x.

360   4.5   Impacts on the nitrogen cycle in California

To our knowledge, this is the first study conducted on NO_2 stomatal deposition to native California tree species, except for *Q. agrifolia* (Delaria et al., 2018). However, there are many measurements of the stomatal conductance of Californian trees. Murray et al. (2019) examined patterns in maximum g_s^w ($max\ g_s^w$) across bioclimatic zones. Among the species they looked at were *A. menziesii*, *A. macrophyllum* and *Q. agrifolia*, for which they measured an average $max\ g_s^w$ of 550 mmol m^{-2} s^{-1},

365   420 mmol m^{-2} s^{-1}, and 390 mmol m^{-2} s^{-1}, respectively. In comparison, our measurements of $max\ g_s^w$ for these species were, respectively, 210 $\pm$ 10 mmol m^{-2} s^{-1}, 400 $\pm$ 100 mmol m^{-2} s^{-1}, and 90 $\pm$ 20 mmol m^{-2} s^{-1}. Our estimates of max g_s^w for *A. menziesii* and *Q. agrifolia* are substantially lower. Maire et al. (2015) determined a maximum stomatal conductance for *A. menziesii* of 150 mmol m^{-2} s^{-1}. For *Quercus* and *Acer* species in similar climate regions, Maire et al. (2015) calculated $max\ g_s^w$ ranging from 103—890 mmol m^{-2} s^{-1} and 112—320 mmol m^{-2} s^{-1}, respectively. Henry et al. (2019) measured a

370   similar maximum stomatal conductance of *Q. agrifolia* to our study of 95 mmol m^{-2} s^{-1}. Maire et al. (2015) also measured a maximum stomatal conductance to water vapor for *P. ponderosa* and *S. sempervirens* of 124 mmol m^{-2} s^{-1} and ~91 mmol m^{-2} s^{-1}, respectively–considerably smaller than the values measured in this study. Ambrose et al. (2010) measured a $max\ g_s^w$ for *S. sempervirens* of 240 m^{-2} s^{-1}, in better agreement with our measurements. *P. ponderosa* stomatal conductance measurements

reported in this study were in very good agreement with the stomatal conductance measured during the BEARPEX-2009
375   campaign in a ponderosa pine dominated forest during a wet year (Min et al., 2014; Delaria and Cohen, 2020). The median
of $max\ g_s^w$ for all four angiosperms we measured was 200 mmol m^{-2} s^{-1} , in good agreement with the 250 mmol m^{-2} s^{-1}
median of all angiosperms in Mediterranean climate regions found by Murray et al. (2019) and the 215 m^{-2} s^{-1} median found
by Maire et al. (2015). Our median for the six gymnosperms measured was 230 m^{-2} s^{-1}, considerably larger than the median
100 m^{-2} s^{-1} $max\ g_s^w$ found by Maire et al. (2015) in Meditteranean climate regions (defined as warm temperature steppe
380   regions as classified by Kottek et al. (2006)).

Overall, the stomatal conductances to water vapor measured in our laboratory experiments falls within the ranges of max
g_s^w measured in previous studies–although significant inconsistencies exist in the current literature. Possible discrepancies may
have resulted from the location each species were measured, growing conditions, ages of the trees, etc. Nevertheless, our NO$_2$
deposition results–and their applicability to California forests–are bolstered by the fact that our $max\ g_s^w$ measurements fall
385   with in the ranges measured for for mature trees in the field. To assess the impact of the lab-measured deposition velocities on
the NO$_x$ cycle in California, we used our measurements of $maxV_d$ and $medV_d$(night) to estimate the flux and lifetime of NO$_x$
to deposition in forests throughout the state during the day and night, respectively (Fig. 7, Fig.8).

The average deposition flux to trees in California was calculated via Eq.11

$$F_{dep} = [NO_2] \times V_d eff \times LAI \times \text{land cover} \tag{11}$$

390   Leaf area index (LAI) data was obtained from MCD15A2H Version 6 Moderate Resolution Imaging Spectroradiometer
(MODIS) Level 4 product (Myneni et al., 2015) (Fig. S3). The NO$_2$ surface concentration over California was obtained from
the OMI satelite using the BEHR product (Laughner et al., 2018) (Fig. S3). Land cover data was obtained from NLCD Land
Cover (CONUS) for 2016 (Yang et al., 2018) (Fig. S1). The land cover data set was modified such that there were only two land
categories: forest and not forest. Only forested sites were considered. Tree counts were obtained from the USDA Forest Service
395   Forestry Inventory Analysis Database (for, 2014) (Fig. S2). For each plot in the Forest Service Inventory that contained more
than 50% of the trees measured in our study, a weighted averaged effective deposition velocity to NO$_2$ ($V_d eff$) was calculated
from the max V_d listed in Table 2 (Fig. S3). Data was interpolated to a 500m grid. The resulting midday fluxes throughout
California are shown in Fig. 7 and midnight fluxes are shown in Fig. 8. The greatest fluxes predicted are near the San Francisco
Bay Area, where there are high NO$_x$ concentrations, and also a relatively high forest LAI for an urban region (Fig. S3). Similar
400   hotspots can be seen near Los Angeles in the inland chaparral regions. Large fluxes are also predicted in the foothill forest
region of the Sierra Nevada mountain range, where there is a a large LAI, and frequent occurances of *P. sabiniana*, the tree
having the largest V_d (Fig. S2, Fig. S3). Relatively large fluxes occur in this region particularly during the nighttime.

The resulting lifetime of NO$_2$ to deposition is calculated via Eq. 12

$$\tau_{dep} = PBL (V_d eff \times LAI \times \text{land cover})^{-1} \tag{12}$$

405   where PBL is the planetary boundary layer height. The lifetimes to deposition during the day for a uniform PBL height of 1
km are shown in Fig. 7. In forested regions the lifetime to deposition is approximately 10 hrs. This is especially significant in

the near-urban San Francisco Bay, where deposition is competitive with the chemical sinks of HNO_3 and $RONO_2$ formation, which typically represent a lifetime to NO_x loss of 2-11 hrs (e.g., Nunnermacker et al., 2000; Dillon et al., 2002; Alvarado et al., 2010; Valin et al., 2013; Romer et al., 2016; Laughner and Cohen, 2019). The lifetimes to deposition during the day

410   for a uniform PBL height of 100 m are shown in Fig. 8. With a reduced boundary layer during the night, the lifetime to NO_x to deposition is on the same order as the deposition lifetime during the day (10—100 hr), representing a very significant permanent loss of NO_x from the atmosphere when compared with the overall NO_x lifetime at night (Brown et al., 2004, 2006; Crowley et al., 2010).

5   Conclusions

415   We present measurements assessing the relative effects of stomatal diffusion and mesophyllic processing of NO_2 on the uptake rate of NO_2. We find that the deposition velocity of NO_2 is essentially equal to the stomatal conductance to NO_2 under conditions of drought, excess soil nitrogen, variations in vapor pressure deficit, and in both the day and night. We find no evidence of any emission of NO_2 from leaves. NO_2 foliar exchange is thus uni-directional and variations are driven–from an atmospheric perspective–nearly entirely by the rate of diffusion through open stomata. This opens the possibility of using direct

420   measurements of stomatal conductance, known relationships of the effects of environmental conditions on stomatal opening, as well as indirect measurements, such as satellite solar-induced fluorescence data to infer NO_x foliar exchange. Additionally, we find significant differences in deposition velocities between species, reflecting differences in maximum stomatal conductance measurements that have been found by a number of previous studies (e.g., Ambrose et al., 2010; Maire et al., 2015; Henry et al., 2019; Murray et al., 2019). This diversity is not reflected in current atmosphric models, and may have a meaningful

425   impact on estimates of regional NO_x fluxes and lifetimes. Our observations of stomatal opening in the absence of light also suggests foliar deposition serves as a large and important sink of NO_x during the night. These findings not only have important implications for NO_x chemistry, but are also relevant for the atmosphere-biosphere exchange of other gasses, such as CO_2 and biogenic volatile organic compounds.

Author contributions.   ERD and BKP designed the experimental setup and ERD, BKP, and AXL collected all NO_2 exchange data. BKP and

430   ERD designed methods and collected data for nitrogen fertilization experiments. ERD and AXL designed methods and collected data for drought stress experiments. ERD performed data analysis, with assistance from AXL. ERD prepared the manuscript in consultation with RCC. RCC supervised the project.

Competing interests.   The authors declare that they have no conflict of interest.

Data availability.   The data collected in this study can be obtained from the authors upon request.

435 *Acknowledgements.* We would like to thank Dr. Stephen Decina for his assistance in designing methods for soil ammonium and nitrate measurements. We would also like to acknowledge Dr. Robert Skelton for consultation on drought stressing trees and for allowing us to borrow a pressure chamber instrument for use in this study.

References

Forest Inventory and Analysis. 2014. The Forest Inventory and Analysis Database: Database description and user guide version 6.0.1 for Phase 3, http://www.fia.fs.fed.us/library/database-documentation/, 2014.

Alvarado, M. J., Logan, J. A., Mao, J., Apel, E., Riemer, D., Blake, D., Cohen, R. C., Min, K.-E., Perring, A. E., Browne, E. C., Wooldridge, P. J., Diskin, G. S., Sachse, G. W., Fuelberg, H., Sessions, W. R., Harrigan, D. L., Huey, G., Liao, J., Case-Hanks, A., Jimenez, J. L., Cubison, M. J., Vay, S. A., Weinheimer, A. J., Knapp, D. J., Montzka, D. D., Flocke, F. M., Pollack, I. B., Wennberg, P. O., Kurten, A., Crounse, J., Clair, J. M. S., Wisthaler, A., Mikoviny, T., Yantosca, R. M., Carouge, C. C., and Le Sager, P.: Nitrogen oxides and PAN in plumes from boreal fires during ARCTAS-B and their impact on ozone: an integrated analysis of aircraft and satellite observations, Atmospheric Chemistry and Physics, 10, 9739–9760, https://doi.org/10.5194/acp-10-9739-2010, https://www.atmos-chem-phys.net/10/9739/2010/, 2010.

Ambrose, A. R., Sillett, S. C., Koch, G. W., Van Pelt, R., Antoine, M. E., and Dawson, T. E.: Effects of height on treetop transpiration and stomatal conductance in coast redwood (Sequoia sempervirens), Tree Physiology, 30, 1260–1272, https://doi.org/10.1093/treephys/tpq064, https://doi.org/10.1093/treephys/tpq064, 2010.

Ammann, M., von Ballmoos, P., Stalder, M., Suter, M., and Brunold, C.: Uptake and assimilation of atmospheric NO2 — N by spruce needles (Picea abies): A field study, Water Air and Soil Pollution, 85, 1497–1502, https://doi.org/10.1007/BF00477193, 1995.

Amnuaylojaroen, T., Barth, M. C., Emmons, L. K., Carmichael, G. R., Kreasuwun, J., Prasitwattanaseree, S., and Chantara, S.: Effect of different emission inventories on modeled ozone and carbon monoxide in Southeast Asia, Atmospheric Chemistry and Physics, 14, 12 983–13 012, https://doi.org/10.5194/acp-14-12983-2014, https://www.atmos-chem-phys.net/14/12983/2014/, 2014.

Andrews, M.: The partitioning of nitrate assimilation between root and shoot of higher plants, Plant, Cell & Environment, 9, 511–519, https://doi.org/10.1111/1365-3040.ep11616228, https://onlinelibrary.wiley.com/doi/abs/10.1111/1365-3040.ep11616228, 1986.

Bahrun, A., Jensen, C. R., Asch, F., and Mogensen, V. O.: Drought-induced changes in xylem pH, ionic composition, and ABA concentration act as early signals in field-grown maize (Zea mays L.), Journal of Experimental Botany, 53, 251–263, https://doi.org/10.1093/jexbot/53.367.251, 2002.

Baldocchi, D. D., Hicks, B. B., and Camara, P.: A canopy stomatal resistance model for gaseous deposition to vegetated surfaces, Atmospheric Environment (1967), 21, 91 – 101, https://doi.org/https://doi.org/10.1016/0004-6981(87)90274-5, http://www.sciencedirect.com/science/article/pii/0004698187902745, 1987.

Breuninger, C., Oswald, R., Kesselmeier, J., and Meixner, F. X.: The dynamic chamber method: trace gas exchange fluxes (NO, NO_2, O_3) between plants and the atmosphere in the laboratory and in the field, Atmospheric Measurement Techniques, 5, 955–989, https://doi.org/10.5194/amt-5-955-2012, https://www.atmos-meas-tech.net/5/955/2012/, 2012.

Breuninger, C., Meixner, F. X., and Kesselmeier, J.: Field investigations of nitrogen dioxide (NO_2) exchange between plants and the atmosphere, Atmospheric Chemistry and Physics, 13, 773–790, https://doi.org/10.5194/acp-13-773-2013, https://www.atmos-chem-phys.net/13/773/2013/, 2013.

Brown, S. S., Dibb, J. E., Stark, H., Aldener, M., Vozella, M., Whitlow, S., Williams, E. J., Lerner, B. M., Jakoubek, R., Middlebrook, A. M., DeGouw, J. A., Warneke, C., Goldan, P. D., Kuster, W. C., Angevine, W. M., Sueper, D. T., Quinn, P. K., Bates, T. S., Meagher, J. F., Fehsenfeld, F. C., and Ravishankara, A. R.: Nighttime removal of NOx in the summer marine boundary layer, Geophysical Research Letters, 31, https://doi.org/10.1029/2004GL019412, 2004.

Brown, S. S., Ryerson, T. B., Wollny, A. G., Brock, C. A., Peltier, R., Sullivan, A. P., Weber, R. J., Dubé, W. P., Trainer, M., Meagher, J. F., Fehsenfeld, F. C., and Ravishankara, A. R.: Variability in Nocturnal Nitrogen Oxide Processing and Its Role in Regional Air Quality, Science, 311, 67–70, https://doi.org/10.1126/science.1120120, 2006.

Chaparro-Suarez, I., Meixner, F., and Kesselmeier, J.: Nitrogen dioxide (NO2) uptake by vegetation controlled by atmospheric concentrations and plant stomatal aperture, Atmospheric Environment, 45, 5742 – 5750, https://doi.org/https://doi.org/10.1016/j.atmosenv.2011.07.021, http://www.sciencedirect.com/science/article/pii/S1352231011007461, 2011.

Chen, J., Wu, F.-H., Liu, T.-W., Chen, L., Xiao, Q., Dong, X.-J., He, J.-X., Pei, Z.-M., and Zheng, H.-L.: Emissions of nitric oxide from 79 plant species in response to simulated nitrogen deposition, Environmental Pollution, 160, 192 – 200, https://doi.org/https://doi.org/10.1016/j.envpol.2011.09.007, http://www.sciencedirect.com/science/article/pii/S0269749111005136, 2012.

Crowley, J. N., Schuster, G., Pouvesle, N., Parchatka, U., Fischer, H., Bonn, B., Bingemer, H., and Lelieveld, J.: Nocturnal nitrogen oxides at a rural mountain-site in south-western Germany, Atmospheric Chemistry and Physics, 10, 2795–2812, https://doi.org/10.5194/acp-10-2795-2010, https://www.atmos-chem-phys.net/10/2795/2010/, 2010.

Crowley, J. N., Pouvesle, N., Phillips, G. J., Axinte, R., Fischer, H., Petäjä, T., Nölscher, A., Williams, J., Hens, K., Harder, H., Martinez-Harder, M., Novelli, A., Kubistin, D., Bohn, B., and Lelieveld, J.: Insights into HO_x and RO_x chemistry in the boreal forest via measurement of peroxyacetic acid, peroxyacetic nitric anhydride (PAN) and hydrogen peroxide, Atmospheric Chemistry and Physics, 18, 13 457–13 479, https://doi.org/10.5194/acp-18-13457-2018, https://www.atmos-chem-phys.net/18/13457/2018/, 2018.

Crutzen, P. J.: The Role of NO and NO2 in the Chemistry of the Troposphere and Stratosphere, Annual Review of Earth and Planetary Sciences, 7, 443–472, https://doi.org/10.1146/annurev.ea.07.050179.002303, https://doi.org/10.1146/annurev.ea.07.050179.002303, 1979.

Dawson, T. E., Burgess, S. S. O., Tu, K. P., Oliveira, R. S., Santiago, L. S., Fisher, J. B., Simonin, K. A., and Ambrose, A. R.: Nighttime transpiration in woody plants from contrasting ecosystems, Tree Physiology, 27, 561–575, https://doi.org/10.1093/treephys/27.4.561, https://doi.org/10.1093/treephys/27.4.561, 2007.

Decina, S. M., Templer, P. H., Hutyra, L. R., Gately, C. K., and Rao, P.: Variability, drivers, and effects of atmospheric nitrogen inputs across an urban area: Emerging patterns among human activities, the atmosphere, and soils, Science of The Total Environment, 609, 1524 – 1534, https://doi.org/https://doi.org/10.1016/j.scitotenv.2017.07.166, http://www.sciencedirect.com/science/article/pii/S0048969717318697, 2017.

Delaria, E. R. and Cohen, R. C.: A model-based analysis of foliar NO_x deposition, Atmospheric Chemistry and Physics, 20, 2123–2141, https://doi.org/10.5194/acp-20-2123-2020, 2020.

Delaria, E. R., Vieira, M., Cremieux, J., and Cohen, R. C.: Measurements of NO and NO_2 exchange between the atmosphere and *Quercus agrifolia*, Atmospheric Chemistry and Physics, 18, 14 161–14 173, https://doi.org/10.5194/acp-18-14161-2018, https://www.atmos-chem-phys.net/18/14161/2018/, 2018.

Dillon, M. B., Lamanna, M. S., Schade, G. W., Goldstein, A. H., and Cohen, R. C.: Chemical evolution of the Sacramento urban plume: Transport and oxidation, Journal of Geophysical Research: Atmospheres, 107, ACH 3–1–ACH 3–15, https://doi.org/10.1029/2001JD000969, https://agupubs.onlinelibrary.wiley.com/doi/abs/10.1029/2001JD000969, 2002.

Drake, P. L., Froend, R. H., and Franks, P. J.: Smaller, faster stomata: scaling of stomatal size, rate of response, and stomatal conductance, Journal of Experimental Botany, 64, 495–505, https://doi.org/10.1093/jxb/ers347, https://doi.org/10.1093/jxb/ers347, 2013.

Fast, J. D., Allan, J., Bahreini, R., Craven, J., Emmons, L., Ferrare, R., Hayes, P. L., Hodzic, A., Holloway, J., Hostetler, C., Jimenez, J. L., Jonsson, H., Liu, S., Liu, Y., Metcalf, A., Middlebrook, A., Nowak, J., Pekour, M., Perring, A., Russell, L., Sedlacek, A., Seinfeld, J., Setyan,

A., Shilling, J., Shrivastava, M., Springston, S., Song, C., Subramanian, R., Taylor, J. W., Vinoj, V., Yang, Q., Zaveri, R. A., and Zhang, Q.: Modeling regional aerosol and aerosol precursor variability over California and its sensitivity to emissions and long-range transport during the 2010 CalNex and CARES campaigns, Atmospheric Chemistry and Physics, 14, 10 013–10 060, https://doi.org/10.5194/acp-14-10013-2014, https://www.atmos-chem-phys.net/14/10013/2014/, 2014.

Fisher, J. B., Baldocchi, D. D., Misson, L., Dawson, T. E., and Goldstein, A. H.: What the towers don't see at night: nocturnal sap flow in trees and shrubs at two AmeriFlux sites in California, Tree Physiology, 27, 597–610, https://doi.org/10.1093/treephys/27.4.597, https://doi.org/10.1093/treephys/27.4.597, 2007.

Hari, P., Raivonen, M., Vesala, T., Munger, J., Pilegaard, K., and Kulmala, M.: Ultraviolet light and leaf emission of NOx, Nature, 422, 134–134, https://doi.org/10.1038/422134a, 2003.

Heidari, B., Matre, P., Nemie-Feyissa, D., Meyer, C., Rognli, O. A., Møller, S. G., and Lillo, C.: Protein Phosphatase 2A B55 and A Regulatory Subunits Interact with Nitrate Reductase and Are Essential for Nitrate Reductase Activation, Plant Physiology, 156, 165–172, https://doi.org/10.1104/pp.111.172734, http://www.plantphysiol.org/content/156/1/165, 2011.

Henry, C. L., John, G. P., Pan, R., Bartlett, M. K., Fletcher, L. R., Scoffoni, C., and Sack, L.: A stomatal safety-efficiency trade-off constrains responses to leaf dehydration, in: Nature Communications, 2019.

Hereid, D. and Monson, R.: Nitrogen Oxide Fluxes between Corn (Zea mays L.) Leaves and the Atmosphere, Atmospheric Environment, 35, 975–983, https://doi.org/10.1016/S1352-2310(00)00342-3, 2001.

Jacob, D. J. and Wofsy, S. C.: Budgets of reactive nitrogen, hydrocarbons, and ozone over the Amazon forest during the wet season, Journal of Geophysical Research: Atmospheres, 95, 16 737–16 754, https://doi.org/10.1029/JD095iD10p16737, https://agupubs.onlinelibrary.wiley.com/doi/abs/10.1029/JD095iD10p16737, 1990.

Joensuu, J., Raivonen, M., Kieloaho, A.-J., Altimir, N., Kolari, P., Sarjala, T., and Bäck, J.: Does nitrate fertilization induce nox emission from scots pine (p. sylvestris) shoots?, Plant and Soil, 388, 283–295, https://doi.org/10.1007/s11104-014-2328-x, 2014.

Johansson, C.: Pine forest: a negligible sink for atmospheric NOx in rural Sweden, Tellus B, 39B, 426–438, https://doi.org/10.1111/j.1600-0889.1987.tb00204.x, https://onlinelibrary.wiley.com/doi/abs/10.1111/j.1600-0889.1987.tb00204.x, 1987.

Kolb, P. and Robberecht, R.: High temperature and drought stress effects on survival of Pinus ponderosa seedlings, Tree physiology, 16, 665–72, https://doi.org/10.1093/treephys/16.8.665, 1996.

Kottek, M., Grieser, J., Beck, C., Rudolf, B., and Rubel, F.: World Map of the Köppen-Geiger Climate Classification Updated, Meteorologische Zeitschrift, 15, 259–263, https://doi.org/10.1127/0941-2948/2006/0130, 2006.

Laughner, J., Zhu, Q., and Cohen, R.: Berkeley High Resolution (BEHR) OMI NO2 - Gridded pixels, daily profiles, v5, UC Berkeley, Dataset, https://doi.org/10.6078/D12D5X, 2018.

Laughner, J. L. and Cohen, R. C.: Direct observation of changing NOx lifetime in North American cities, Science, 366, 723–727, https://doi.org/10.1126/science.aax6832, https://science.sciencemag.org/content/366/6466/723, 2019.

Lerdau, M. T., Munger, J. W., and Jacob, D. J.: The NO2 Flux Conundrum, Science, 289, 2291–2293, https://doi.org/10.1126/science.289.5488.2291, https://science.sciencemag.org/content/289/5488/2291, 2000.

Lillo, C.: Signalling cascades integrating light-enhanced nitrate metabolism, Biochemical Journal, 415, 11–19, https://doi.org/10.1042/BJ20081115, https://doi.org/10.1042/BJ20081115, 2008.

Maherali, H. and DeLucia, E. H.: Xylem conductivity and vulnerability to cavitation of ponderosa pine growing in contrasting climates, Tree Physiology, 20, 859–867, https://doi.org/10.1093/treephys/20.13.859, 2000.

Maire, V., Wright, I. J., Prentice, I. C., Batjes, N. H., Bhaskar, R., van Bodegom, P. M., Cornwell, W. K., Ellsworth, D., Niinemets, ,
550   Ordonez, A., Reich, P. B., and Santiago, L. S.: Global effects of soil and climate on leaf photosynthetic traits and rates, Global Ecology
       and Biogeography, 24, 706–717, https://doi.org/10.1111/geb.12296, https://onlinelibrary.wiley.com/doi/abs/10.1111/geb.12296, 2015.

Massman, W.: A review of the molecular diffusivities of H_2O, CO_2, CH_4, CO, O_3, SO_2, NH_3, N_2O, NO, and NO_2 in air, O_2 and N_2 near
       STP, Atmospheric Environment, 32, 1111 – 1127, https://doi.org/https://doi.org/10.1016/S1352-2310(97)00391-9, 1998.

Min, K.-E., Pusede, S. E., Browne, E. C., LaFranchi, B. W., and Cohen, R. C.: Eddy covariance fluxes and vertical concentration gradient
555   measurements of NO and NO_2 over a ponderosa pine ecosystem: observational evidence for within-canopy chemical removal of NO_x,
       Atmospheric Chemistry and Physics, 14, 5495–5512, https://doi.org/10.5194/acp-14-5495-2014, https://www.atmos-chem-phys.net/14/
       5495/2014/, 2014.

Murray, M., Soh, W. K., Yiotis, C., Batke, S., Parnell, A. C., Spicer, R. A., Lawson, T., Caballero, R., Wright, I. J., Purcell, C., and McElwain,
       J. C.: Convergence in Maximum Stomatal Conductance of C3 Woody Angiosperms in Natural Ecosystems Across Bioclimatic Zones,
560   Frontiers in Plant Science, 10, 558, https://doi.org/10.3389/fpls.2019.00558, https://www.frontiersin.org/article/10.3389/fpls.2019.00558,
       2019.

Musselman, R. C. and Minnick, T. J.: Nocturnal stomatal conductance and ambient air quality standards for ozone, Atmospheric Envi-
       ronment, 34, 719 – 733, https://doi.org/https://doi.org/10.1016/S1352-2310(99)00355-6, http://www.sciencedirect.com/science/article/pii/
       S1352231099003556, 2000.

565   Myneni, R., Knyazikhin, Y., and Park, T.: MCD15A2H MODIS/Terra+Aqua Leaf Area Index/FPAR 8-day L4 Global 500m SIN Grid V006
       [Data set].NASA EOSDIS Land Processes DAAC, https://doi.org/10.5067/MODIS/MCD15A2H.006, 2015.

Ng, N. L., Brown, S. S., Archibald, A. T., Atlas, E., Cohen, R. C., Crowley, J. N., Day, D. A., Donahue, N. M., Fry, J. L., Fuchs, H., Griffin,
       R. J., Guzman, M. I., Herrmann, H., Hodzic, A., Iinuma, Y., Jimenez, J. L., Kiendler-Scharr, A., Lee, B. H., Luecken, D. J., Mao, J.,
       McLaren, R., Mutzel, A., Osthoff, H. D., Ouyang, B., Picquet-Varrault, B., Platt, U., Pye, H. O. T., Rudich, Y., Schwantes, R. H., Shiraiwa,
570   M., Stutz, J., Thornton, J. A., Tilgner, A., Williams, B. J., and Zaveri, R. A.: Nitrate radicals and biogenic volatile organic compounds:
       oxidation, mechanisms, and organic aerosol, Atmospheric Chemistry and Physics, 17, 2103–2162, https://doi.org/10.5194/acp-17-2103-
       2017, https://www.atmos-chem-phys.net/17/2103/2017/, 2017.

Nunnermacker, L. J., Kleinman, L. I., Imre, D., Daum, P. H., Lee, Y.-N., Lee, J. H., Springston, S. R., Newman, L., and Gillani, N.:
       NO y lifetimes and O3 production efficiencies in urban and power plant plumes: Analysis of field data, Journal of Geophysical Re-
575   search: Atmospheres, 105, 9165–9176, https://doi.org/10.1029/1999JD900753, https://agupubs.onlinelibrary.wiley.com/doi/abs/10.1029/
       1999JD900753, 2000.

Okano, K. and Totsuka, T.: Absorption of nitrogen dioxide by sunflower plants grown at various levels of nitrate, New Phytologist,
       102, 551–562, https://doi.org/10.1111/j.1469-8137.1986.tb00831.x, https://nph.onlinelibrary.wiley.com/doi/abs/10.1111/j.1469-8137.
       1986.tb00831.x, 1986.

580   Pape, L., Ammann, C., Nyfeler-Brunner, A., Spirig, C., Hens, K., and Meixner, F. X.: An automated dynamic chamber system
       for surface exchange measurement of non-reactive and reactive trace gases of grassland ecosystems, Biogeosciences, 6, 405–429,
       https://doi.org/10.5194/bg-6-405-2009, https://www.biogeosciences.net/6/405/2009/, 2009.

Park, J. Y. and Lee, Y. N.: Solubility and decomposition kinetics of nitrous acid in aqueous solution, The Journal of Physical Chemistry, 92,
       6294–6302, https://doi.org/10.1021/j100333a025, https://doi.org/10.1021/j100333a025, 1988.

585   Pharis, R.: Comparative Drought Resistance of Five Conifers and Foliage Moisture Content as a Viability Index, Ecology, 47, 211,
       https://doi.org/10.2307/1933767, 1966.

Pietilainen, P. and Lahdesmaki, P.: Effect of various concentrations of potassium nitrate and ammonium sulphate on nitrate reductase activity in the roots and needles of Scots pine seedlings in N Finland, Annales Botanici Fennici, 25, 201–206, http://www.jstor.org/stable/23725723, 1988.

590 Raivonen, M., Bonn, B., Sanz, M. J., Vesala, T., Kulmala, M., and Hari, P.: UV-induced NOy emissions from Scots pine: Could they originate from photolysis of deposited HNO3?, Atmospheric Environment, 40, 6201 – 6213, https://doi.org/https://doi.org/10.1016/j.atmosenv.2006.03.063, http://www.sciencedirect.com/science/article/pii/S135223100600522X, 2006.

Ramge, P., Badeck, F.-W., Plochl, M., and Kohlmaier, G. H.: Apoplastic antioxidants as decisive elimination factors within the uptake
595 process of nitrogen dioxide into leaf tissues, New Phytologist, 125, 771–785, https://doi.org/10.1111/j.1469-8137.1993.tb03927.x, https://nph.onlinelibrary.wiley.com/doi/abs/10.1111/j.1469-8137.1993.tb03927.x, 1993.

Rogers, H. H., Jeffries, H. E., and Witherspoon, A. M.: Measuring Air Pollutant Uptake by Plants: Nitrogen Dioxide, Journal of Environmental Quality, 8, 551–557, https://doi.org/10.2134/jeq1979.00472425000800040022x, https://acsess.onlinelibrary.wiley.com/doi/abs/10.2134/jeq1979.00472425000800040022x, 1979.

600 Romer, P. S., Duffey, K. C., Wooldridge, P. J., Allen, H. M., Ayres, B. R., Brown, S. S., Brune, W. H., Crounse, J. D., de Gouw, J., Draper, D. C., Feiner, P. A., Fry, J. L., Goldstein, A. H., Koss, A., Misztal, P. K., Nguyen, T. B., Olson, K., Teng, A. P., Wennberg, P. O., Wild, R. J., Zhang, L., and Cohen, R. C.: The lifetime of nitrogen oxides in an isoprene-dominated forest, Atmospheric Chemistry and Physics, 16, 7623–7637, https://doi.org/10.5194/acp-16-7623-2016, https://www.atmos-chem-phys.net/16/7623/2016/, 2016.

Rondón, A. and Granat, L.: Studies on the dry deposition of NO2 to coniferous species at low NO2 concentrations, Tellus B: Chemical and
605 Physical Meteorology, 46, 339–352, https://doi.org/10.3402/tellusb.v46i5.15809, https://doi.org/10.3402/tellusb.v46i5.15809, 1994.

Sarjala, T.: Effect of mycorrhiza and nitrate nutrition on nitrate reductase activity in Scots pine seedlings, Physiologia Plantarum, 81, 89–94, https://doi.org/10.1111/j.1399-3054.1991.tb01718.x, https://onlinelibrary.wiley.com/doi/abs/10.1111/j.1399-3054.1991.tb01718.x, 1991.

Schneider, C. A., R. W. S. and Eliceiri, K. W.: A Preliminary multiple resistance routine for deriving dry deposition velocities from measured quantities, Nature Methods, 9, 671–675, https://doi.org/10.1038/nmeth.2089, 2012.

610 Sims, G. K., Ellsworth, T. R., and Mulvaney, R. L.: Microscale determination of inorganic nitrogen in water and soil extracts, Communications in Soil Science and Plant Analysis, 26, 303–316, https://doi.org/10.1080/00103629509369298, https://doi.org/10.1080/00103629509369298, 1995.

Skamarock, W. C., K. J. B. D. J. G. D. O. B. D. M. D. M. G. H. X.-Y. W. W. and Powers, J. G.: A Description of the Advanced Research WRF Version 3, Tech. rep., National Center for Atmospheric Res., https://doi.org/10.5065/D68S4MVH, 2008.

615 Sparks, J., Monson, R., Sparks, K., and Lerdau, M.: Leaf uptake of nitrogen dioxide (NO2) in a tropical wet forest: Implications for tropospheric chemistry, Oecologia, 127, 214–221, https://doi.org/10.1007/s004420000594, 2001.

Sparks, J. P., Roberts, J. M., and Monson, R. K.: The uptake of gaseous organic nitrogen by leaves: A significant global nitrogen transfer process, Geophysical Research Letters, 30, https://doi.org/10.1029/2003GL018578, https://agupubs.onlinelibrary.wiley.com/doi/abs/10.1029/2003GL018578, 2003.

620 Teklemmariam, T. and Sparks, J.: Leaf fluxes of NO and NO2 in four herbaceous plant species: The role of ascorbic acid, Atmospheric Environment, 40, 2235–2244, https://doi.org/10.1016/j.atmosenv.2005.12.010, 2006.

Thornton, J. A., Wooldridge, P. J., and Cohen, R. C.: Atmospheric NO2: In Situ Laser-Induced Fluorescence Detection at Parts per Trillion Mixing Ratios, Analytical Chemistry, 72, 528–539, https://doi.org/10.1021/ac9908905, pMID: 10695138, 2000.

Tischner, R.: Nitrate uptake and reduction in higher and lower plants, Plant, Cell & Environment, 23, 1005–1024, https://doi.org/10.1046/j.1365-3040.2000.00595.x, https://onlinelibrary.wiley.com/doi/abs/10.1046/j.1365-3040.2000.00595.x, 2000.

Valin, L. C., Russell, A. R., and Cohen, R. C.: Variations of OH radical in an urban plume inferred from NO2 column measurements, Geophysical Research Letters, 40, 1856–1860, https://doi.org/10.1002/grl.50267, https://agupubs.onlinelibrary.wiley.com/doi/abs/10.1002/grl.50267, 2013.

von Caemmerer, S. and Farquhar, G. D.: Some relationships between the biochemistry of photosynthesis and the gas exchange of leaves, Planta, 153, 376–387, https://doi.org/10.1007/BF00384257, https://doi.org/10.1007/BF00384257, 1981.

Wolfe, G. M., Thornton, J. A., Yatavelli, R. L. N., McKay, M., Goldstein, A. H., LaFranchi, B., Min, K.-E., and Cohen, R. C.: Eddy covariance fluxes of acyl peroxy nitrates (PAN, PPN and MPAN) above a Ponderosa pine forest, Atmospheric Chemistry and Physics, 9, 615–634, https://doi.org/10.5194/acp-9-615-2009, https://www.atmos-chem-phys.net/9/615/2009/, 2009.

Yang, L., Jin, S., Danielson, P., Homer, C., Gass, L., Bender, S. M., Case, A., Costello, C., Dewitz, J., Fry, J., Funk, M., Granneman, B., Liknes, G. C., Rigge, M., and Xian, G.: A new generation of the United States National Land Cover Database: Requirements, research priorities, design, and implementation strategies, ISPRS Journal of Photogrammetry and Remote Sensing, 146, 108 – 123, https://doi.org/https://doi.org/10.1016/j.isprsjprs.2018.09.006, http://www.sciencedirect.com/science/article/pii/S092427161830251X, 2018.

Zhang, L., Moran, M., Makar, P., Brook, J., and Gong, S.: Modelling gaseous dry deposition in AURAMS – A Unified Regional Air-quality Modelling System, Atmospheric Environment, 36, 537–560, https://doi.org/10.1016/S1352-2310(01)00447-2, 2002.
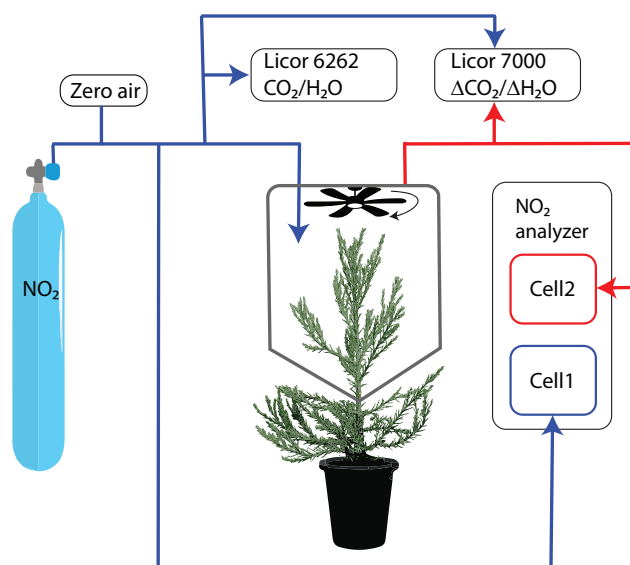
Figure 1. Figure of instrumental setup. Blue lines show the flow of gas that enters the chamber and red lines show the flow of gas sampled from the chamber.
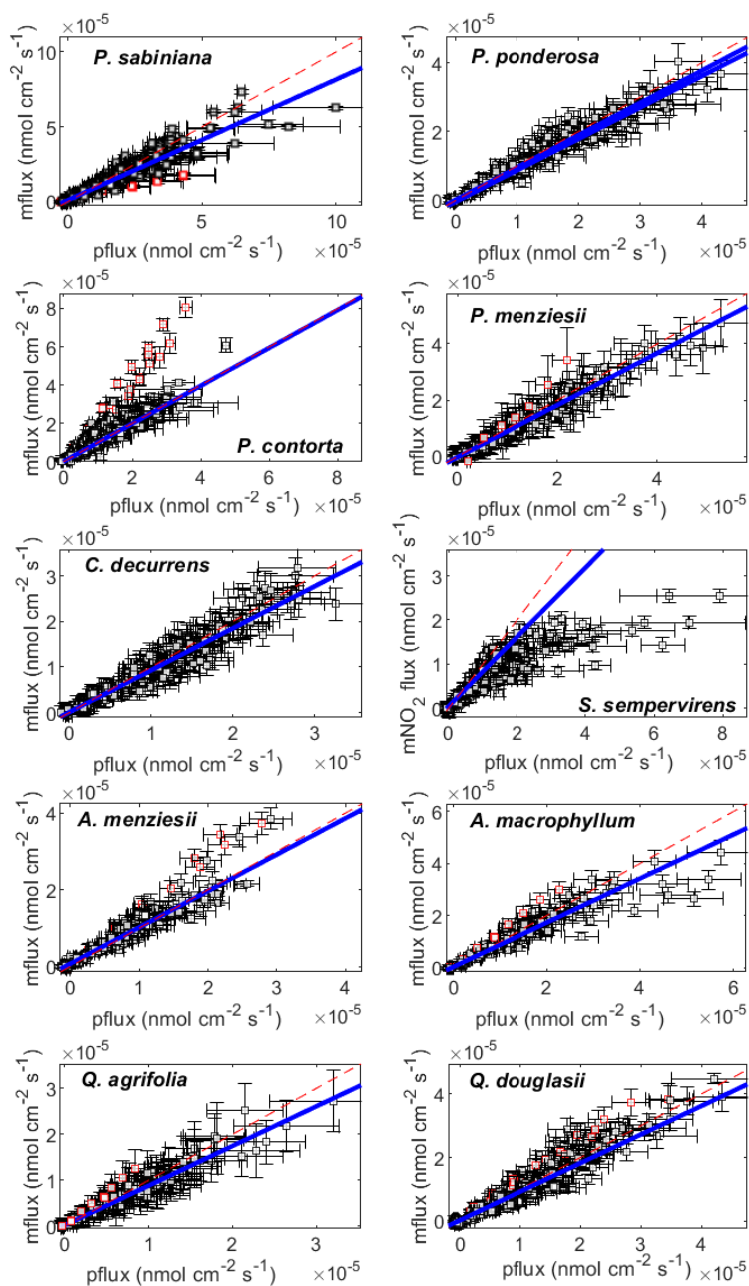
Figure 2. Measured fluxes (mflux) plotted against stomatal-limited predicted fluxes (pflux). Blue solid lines are the linear fit to data. Red lines are the 1:1 line. Error bars for the measured fluxes are calculated by propagating uncertainty in the measured NO_2 mixing ratios, the flow rate, and the leaf area (Eq. 1). Error bars for the predicted fluxes are calculated by propagating uncertainties in the measured NO_2 mixing ratios and the total conductance (Eq. 8). Red markers indicate data determined to be outliers by a generalized extreme studentized deviate test for outliers.
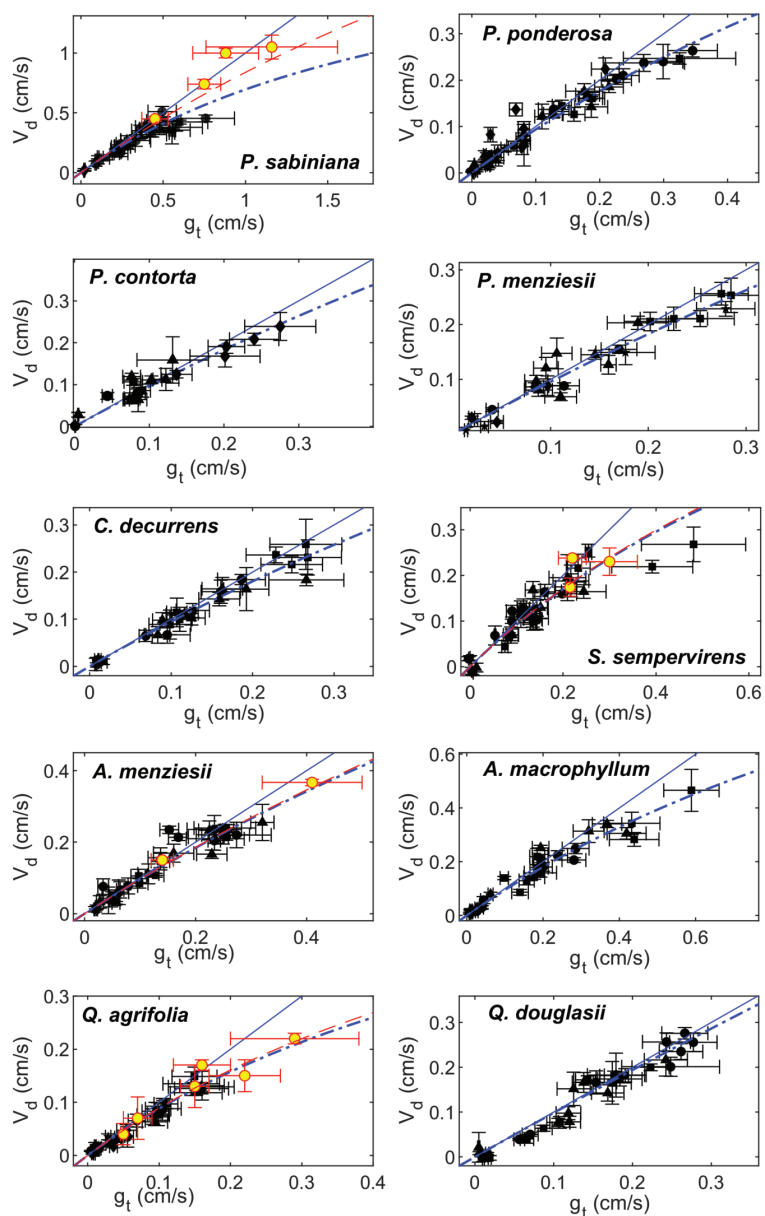
Figure 3. Deposition velocities plotted against measured stomatal conductances to NO_2. Black markers represent measurements in zero air and red-yellow markers are measurements in helium. Solid blue lines are the 1:1 line and dashed blue lines are error weighted fits to the resistance model using only measurements in zero air (Eq. 4). Fits to the resistance model including data from helium measurements are shown as dashed red lines.
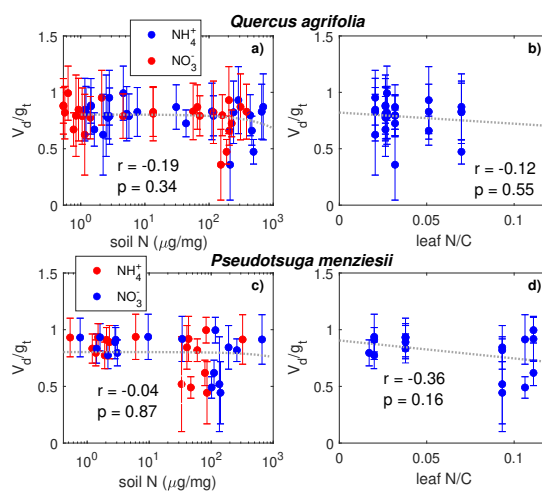
Figure 4. The V_d/g_t ratio is plotted against soil nitrogen concentration in the form of NH_4^+ and NO_3^- for (a) *Q. agrifolia* and (c) *P. menziesii*. The V_d/g_t ratio is plotted against the leaf nitrogen:carbon ratio for (b) *Q. agrifolia* and (d) *P. menziesii*. On each pannel the Pearson's correlation coefficient and the p-value for the slope are shown. The amount of soil and leaf nitrogen has no significant impact on the V_d/g_t ratio.
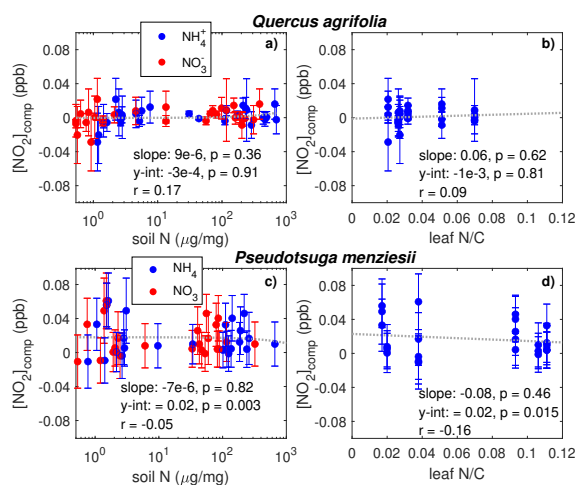
Figure 5. $[NO_2]_{comp}$ is plotted against soil nitrogen concentration in the form of NH_4^+ and NO_3^- for (a) *Q. agrifolia* and (c) *P. menziesii*. $[NO_2]_{comp}$ is plotted against the leaf nitrogen:carbon ratio for (b) *Q. agrifolia* and (d) *P. menziesii*. On each pannel the Pearson's correlation coefficient, the slope, the intercept, and their p-values are shown. The amount of soil and leaf nitrogen has no significant impact on the compensation point.
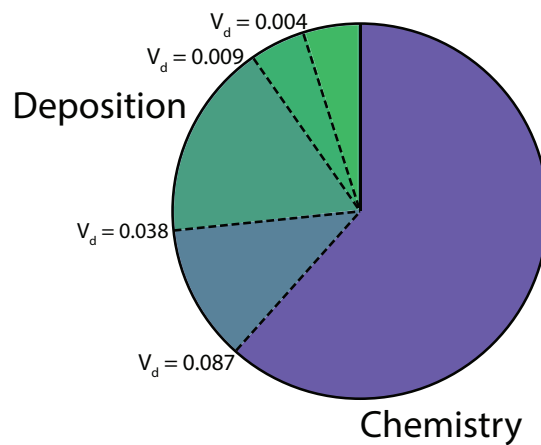
Figure 6. Fraction of NO$_x$ loss to deposition and chemistry (nitric acid, alkyl nitrate, and peroxyacyl nitrate). The four dashed lines between the deposition and chemistry fractions show NO$_x$ loss with a nighttime NO$_2$ deposition velocity of 0.004, 0.009, 0.038, and 0.087 cm s^{-1}. These deposition velocities respectively represent the minimum, first quartile, third quartile, and maximum of the median nighttime deposition velocities measured for the native California trees examined in this study.
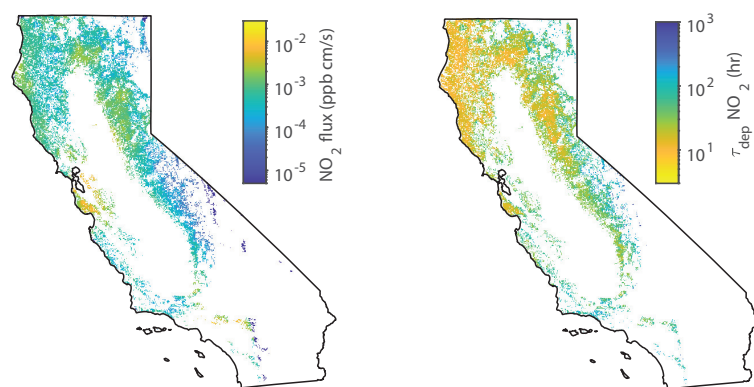
Figure 7. (left) Average midday deposition fluxes of NO_2 to forests in June throughout California. (right) Average midday deposition lifetimes of NO_x assuming a uniform 1 km boundary layer height in June throughout California. White areas are non-forested areas.
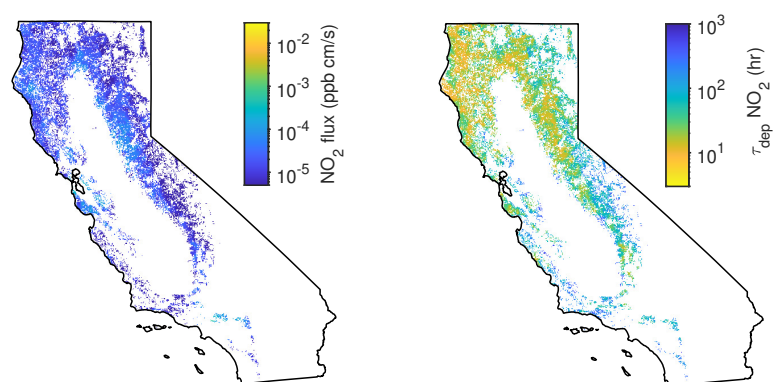
Figure 8. (left) Average midnight deposition fluxes of NO₂ to forests in June throughout California. (right) Average midnight deposition lifetimes of NO_x assuming a uniform 100 m boundary layer height in June throughout California. White areas are non-forested areas.

Table 1. Average soil and leaf nitrogen

tree[a]	soil NH_4^+	soil NO_3^-	leaf N	leaf C
	μg/mg	μg/mg	%	%
QA control	3.0 ± 0.5	3 ± 1	1.1 ± 0.1	47.7 ± 0.2
QA high N	300 ± 60	170 ± 30	2.4 ± 0.5	48.1 ± 0.2
PM control	2.7 ± 0.8	2.0 ± 0.5	1.3 ± 0.2	56 ± 9
PM high N	190 ± 43	80 ± 20	4.7 ± 0.2	45.9 ± 0.4

a. QA is *Q. agrifolia* and PM is *Pseudotsuga menziesii*.

Table 2. Summary of species-dependent foliar deposition results

species	R_m (g_t) s cm^{-1}	R_m (g_s) s cm^{-1}	max[d] V_d cm s^{-1}	max[e] g_t^w cm s^{-1}	median dark V_d mmol m^{-2} s^{-1}	slope[a]	r g_t vs. slope	[NO$_2$]$_{comp}$ ppb
P. sabiniana	0.43±0.06	0.46±0.06	0.51±0.04	500±100	0.087	0.79±0.04	-0.37[c]	-0.03±0.03
P.ponderosa	0.7±0.1	0.69±0.09	0.26±0.01	230±25	0.038	0.91±0.05	-0.72[c]	0.00±0.02
P.contorta	0.5±0.2	0.5±0.2	0.24±0.03	180±30	0.018	0.99±0.03	-0.36[c]	0.00±0.01
P. menziesii	0.30±0.07	0.30±0.06	0.26±0.02	230±20	0.044	0.91±0.04	-0.26	0.02±0.02[b]
C. decurrens	0.4±0.1	0.4±0.1	0.21±0.03	160±20	0.009	0.91±0.02	-0.36[c]	0.00±0.02
S. sempervirens	0.9±0.1	0.9±0.1	0.27±0.04	330±80	0.009	0.60±0.04	-0.43[c]	-0.01±0.02
A. menziesii	0.4±0.1	0.4±0.1	0.26±0.05	210±10	0.037	0.93±0.03	-0.38[c]	-0.02±0.01
A. macrophyllum	0.5±0.1	0.54±0.09	0.47±0.08	400±100	0.017	0.84±0.03	-0.21	-0.02±0.01
Q.agrifolia	1.3±0.3	1.3±0.2	0.15±0.01	90±20	0.008	0.89±0.04	-0.22	0.00±0.01
Q. douglasii	0.2±0.1	0.2±0.1	0.30±0.03	180±20	0.004	0.89±0.04	0.23	-0.01±0.02

a. Slope of measured vs. predicted fluxes (Fig. 2).

b. Statistically significant (α = 0.01) compensation point. Compensation point listed is at limit of detection for the instrument.

c. Statistically significant (α = 0.05) correlation.

e. Maximum stomatal conductance that was observed during our experiments and the error associated with that measurement.

e. Listed maximum g_t^w the maximum stomatal conductance to water vapor that was observed during our experiments and the error associated with the measurement. Units in mmol m^{-2} s^{-1} for ease of comparison with other stomatal conductance studies.

Table 3. Summary of drought stress results

tree[a]	med Ψ_p (IQR) MPa	med g_t (IQR) cm s^{-1}	med V_d (IQR) cm s^{-1}	R_m s cm^{-1}	slope[b]	r[c] g_t vs V_d/g_t	r[c] Ψ_p vs g_t
PP control	-0.60 (0.35)	0.23 (0.17)	0.21 (0.13)	0.69 ± 0.09	0.89 ± 0.02	-0.59[d]	0.651[d]
PP drought	-1.05 (0.53)	0.07 (0.12)	0.06 (0.12)	0.0 ± 0.3	1.0 ± 0.1	-0.10	
CD control	-0.30 (0.30)	0.13 (0.09)	0.12 (0.09)	0.37 ± 0.15	0.95 ± 0.02	-0.11	0.357[d]
CD drought	-0.80 (0.45)	0.06 (0.05)	0.06 (0.05)	1.17 ± 0.38	0.88 ± 0.03	-0.23	

a. PP is *Pinus ponderosa* and CD is *Calocedrus decurrens*

b. Slope of measured vs. predicted fluxes.

c. Pearson correlation coefficients.

d. Statistically significant ($\alpha = 0.05$ correlation).